IET Communications

Special Issue: Advances in Enabling Technologies for Green Communications and Networking

Optimal power dispatch of a centralised electric vehicle battery charging station with renewables

ISSN 1751-8628
Received on 17th June 2017
Revised 11th October 2017
Accepted on 2nd December 2017
E-First on 6th March 2018
doi: 10.1049/iet-com.2017.0610
www.ietdl.org

Wenjin (Jason) Li[1,2], *Xiaoqi Tan*[1], *Bo Sun*[1] ✉, *Danny H. K. Tsang*[1]

[1]*Department of Electronic and Computer Engineering, The Hong Kong University of Science and Technology, Kowloon, Hong Kong*
[2]*Current affiliation: Well Being Digital Limited, Sha Tin, New Territories, Hong Kong*
✉ *E-mail: bsunaa@ust.hk*

Abstract: Historically, transportation electrification has been largely hindered by the limited battery capacity and the long charging time. Battery swapping has emerged as one promising technology to mitigate these problems. A centralised battery charging station (BCS) is responsible for charging depleted batteries (DBs) and providing fully-charged batteries (FBs) for multiple geographically-distributed battery swapping stations (BSSs) so that they can carry out battery swapping services. Facilitated by the recent advancement in sensor and communication technologies, one salient advantage of this centralised approach lies in its convenience to better utilise dual energy sources (i.e. the traditional power grid and local renewable energy generators). This is achieved via optimising the charging processes of a large number of DBs. In this study, the authors propose an optimisation framework for a centralised BCS to minimise the energy cost from the dual energy sources to satisfy the FB demands from multiple BSSs. Particularly, the power dispatch problem in the day-ahead and real-time electricity markets is formulated as a two-stage stochastic optimisation through consideration of the intermittent renewable energy. Numerical simulations show that the proposed optimised power dispatch is capable of achieving cost saving of 76% compared with the benchmark, subject to the limited information available in day-ahead.

1 Introduction

With rising emphasis placed on environmental protection and resource conservation today, transportation and electricity generation still contribute over 60% to the global primary energy demands [1], the majority from fossil sources. Extensive application of electric vehicles (EVs) and renewable energy generation is an inevitable trend [2]. This is increasingly happening in many countries especially for public transportation [3, 4]. Personal ownership is also realised thanks to many major automobile manufacturers such as Tesla [5] and BYD [6]. Such a transition essentially shifts sources of emission from geographically distributed individual vehicles to a few centralised power plants, simplifying pollution control to some extent.

However, the status quo is still far from perfection. Firstly, the electricity used by EVs is still mainly generated from fossil sources in many countries as of today. As a result, pollution might be merely migrated elsewhere without much reduction, violating the main purpose of introducing EVs [7]. Secondly, current battery technology is still incapable of storing enough energy for a medium-to-long-distance trip, so an EV owner has to charge the battery very frequently to alleviate the *range anxiety* (i.e. the fear that an EV would fail to reach its destination due to insufficient energy). Furthermore, the EV would be stuck charging for tens of minutes or even several hours, depending on its charging mode [8] and initial state-of-charge (SOC) level. Such a long duration not only limits the EV's flexibility, reducing the incentive for wider adoption but also increases society cost by demanding more charging facilities to be built with high density in order to make it easy for EV owners to find one.

1.1 Workflow and challenges of battery swapping

To overcome these drawbacks, a battery swapping strategy can be applied [9]. Under this strategy, the batteries in *all* EVs have plug-and-play mounting capabilities through a *unified* interface. At a battery swapping station (BSS), EVs get their depleted batteries (DBs) swapped with fully-charged batteries (FBs) by human staff or automated robots. This is nearly instantaneous compared with hours of in-house charging. Preferably, a BSS should have sufficient inventory of FBs to accommodate random EV arrivals.

Although the DBs can be charged inside the BSS locally as has been considered in our previous work [10], this would complicate the BSS structure, and bring about spatial and safety issues. These are fatal, especially for crowded urban areas. In this regard, we focus on another feasible way in this work, which is to regularly send the DBs to a contracted *centralised* battery charging station (BCS) to produce FBs. This is depicted in Fig. 1. Each contract would specify the FB demands of the participating BSS on a per-time-slot basis, e.g. every one or several hours. The BCS is then responsible for producing and delivering timely and adequate FBs to all of its contracted BSSs. In reality, many municipal authorities in China, such as Hangzhou and Guangzhou [11], have built their electric bus system in such a distributed swapping and centralised charging mechanism. Compared with traditional plug-in charging, battery swapping improves efficiency and flexibility of charging facilities, here the charging bays (CBs) in a BCS. This is because the statistics of EV arrivals no longer directly affect charging scheduling [9]. As a result, both EV owners [12] and grid operators [13] enjoy numerous benefits including but not limited to a fast energy refuelling service and load balancing [14].

In particular, such a structure enables the control centre to easily access and manipulate the system states and parameters using modern sensor and communication technologies. This further opens up possibilities to utilise dual power sources, i.e. the conventional power source (CPS, typically the distribution grid) and the renewable power source (RPS), by optimising the charging process of a large number of DBs. In this way, the green renewable energy is utilised more, fully justifying adoption of EVs [7]. However, in order to achieve this goal, several crucial challenges need to be tackled, namely, the difficulties to accurately predict:

- Renewable energy generation in fine granularity, due to its intermittent and time-variant nature [15].
- Real-time pricing (RTP) of electricity in short term, since the electricity market operates with a very complicated mechanism [16].

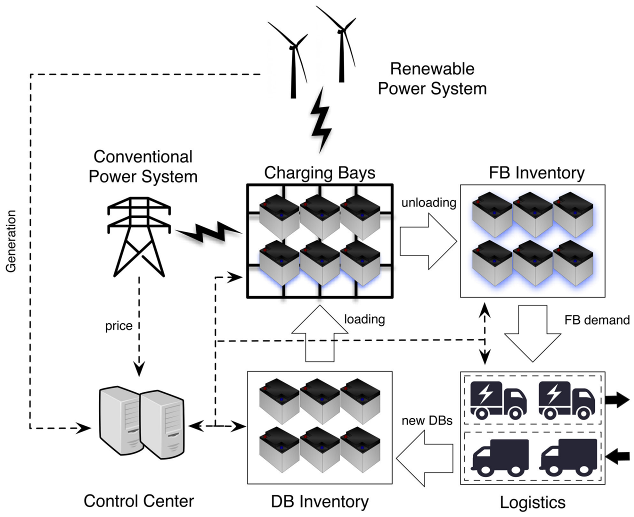

Fig. 1 *System model for the key components of a dual-source BCS.*

Without working around these two problems, blindly integrating renewables would introduce great threats to the stability of EV charging systems as well as the grid via the uncertain amount of available energy [17, 18]. A smart charging scheme shall consider these aspects so that efficiencies in both energy consumption and cost are realised [19, 20]. Hence, in this work, we focus on finding the optimal power dispatch (OPD) to the CPS and the RPS, respectively, in order to minimise the total charging cost subject to the operational constraints and satisfaction of the FB demands.

1.2 Related works

Motivated by the aforementioned benefits, increasing research effort has been put into developing the battery swapping strategy from the perspectives of operation research and power engineering. For instance, Raviv [21] defined the BCS battery charging scheduling as an inventory management problem, simultaneously optimising the profit or cost and satisfying the FB demands. However, the charging rate of each CB was assumed to be fixed. In [22], the optimal battery charging and purchasing strategies were extended from a single BCS to a network of BCSs to balance the short-term operational cost and the long-term investment in batteries. A more recent paper [23] leveraged the queueing network model and formulated a constrained Markov decision process to solve for the optimal charging policy, but that was for the local charging *and* swapping mode instead of centralised charging. All the above works have provided extensive insight into the optimal operation of the battery swapping strategy, yet without considering the integration of renewable generation.

On the other hand, although not much investigation exists in applying renewable energy specifically to the battery swapping strategy, the smart grid community has indeed seen a few related attempts in the broader field of EV charging. For example, a price-incentive model based on the power balance between the renewable generation and the loads was proposed in [24] to coordinate the charging of EVs and the BSS to minimise the total cost of EVs and maximise the profit of the BSS. Zhang *et al.* [25] described the uncertainty of EV arrivals, the intermittence of renewable energy and the variation of the grid power price as independent Markov processes, and minimised the mean waiting time for EVs under the long-term cost constraint. Recently, Jin *et al.* [26] adopted Lyapunov optimisation to avoid having to know the statistics of the underlying processes of renewable energy generation, EV charging demands or extra energy pricing a priori. Despite the above great efforts, to the best of our knowledge, no previous work has addressed any problem specifically on integrating renewable energy into the optimal charging of a *centralized* EV BCS.

1.3 Our contributions

Compared with previous works, our OPD has the following advantages:

- Renewable energy is efficiently integrated to centralised EV battery charging, *without having to know its exact realisation in day-ahead*. This not only reduces the operational cost of the BCS but also avoids underutilisation of the precious renewable energy due to its intermittent generation. It is worth emphasising that *no additional energy storage device* is required under our approach.
- The proposed two-stage stochastic optimisation formulation enables the BCS operator to participate in demand response [27] with high confidence in the day-ahead purchase of grid power as well as quick reaction to RTP fluctuation. For the utility side, having knowledge on the day-ahead commitment of its customers (the BCSs) facilitates more effective infrastructure planning and load forecasting [28].
- The novel model of the BCS operation is simple yet realistic to capture the fundamental physical constraints. As a result, the OPD problem can be solved efficiently with large-size and fine-grained data.

The remainder of this paper is organised as follows. Section 2 models the battery charging process and the system constraints. The OPD is formally formulated as a two-stage stochastic optimisation problem in Section 3, and the sample average approximation (SAA) method is deployed to tackle it. We show the performance evaluation setup and perform a series of case studies using real pricing data in Section 4. They would yield thought-provoking numerical results on the impact of the system parameters under our proposed OPD. Finally, Section 5 draws the conclusion and suggests some future directions of the paper.

2 System model

2.1 Problem statement and assumptions

As illustrated before, the OPD problem requires the power dispatch decisions to be made from the control centre's perspective based on CPS pricing and RPS generation. If the power dispatch decisions were made solely in real-time, the optimality would be largely limited due to unforeseen fluctuations in renewable generation and RTP, but it is generally difficult to accurately predict these as discussed in Section 1.1. Therefore, we suggest decomposing the OPD problem into the following two stages.

2.1.1 Stage 1 – day-ahead commitment.: Now the BCS operator only needs to roughly predict the amount of renewable energy generation and the RTP in each time slot (e.g. each hour) of the coming day. Since the exact realisations of these two stochastic processes are unknown yet, the objective at this stage is to find the optimal purchased day-ahead grid power to minimise the total *expected* charging cost over all possible realisations of them. A purchasing request for grid power for each time slot of the following day is then made in a *day-ahead* manner to the utility company.

2.1.2 Stage 2 – real-time adjustment.: The total available power, i.e. the generated renewable power plus the purchased *day-ahead* grid power, may sometimes be inadequate for the optimal aggregate charging load computed by the OPD. For instance, this may happen when the CBs are rushing for some very urgent FB demands. To compensate for the mismatch, extra grid power has to be purchased in *real-time*. Note that the day-ahead and real-time purchasing markets exhibit distinct pricing behaviours.

On the other hand, if in any time slot the OPD decides that the aggregate charging load should be less than what is available, there would be excess power. Often this is due to poor day-ahead predictions. The utility company can thus buy this amount back at another price level, preferably quite low to discourage excessively large gaps and encourage higher day-ahead accuracy in turn. Since we have assumed no additional energy storage, this is the only means of dealing with the excess amount, if not simply wasted.

Besides the energy cost, also worthy is that a faster charging rate leads to more severe degradation of battery lifetime [29, 30]. Taking into account both concerns, the objective at Stage 2 is to find the optimal aggregate charging rate of the entire BCS to minimise the real-time cost. This consists of the electricity payment for real-time grid power and the battery degradation cost. The day-ahead cost is not covered now because it has already been committed and can no longer be changed. However, given the *day-ahead* commitment, the (bidirectional) *real-time* adjustment is obtained via subtracting the total available power from the desired aggregate charging rate, thus realising the optimal charging rate solved from the OPD.

2.1.3 Assumptions.: For ease of illustration, the scheduling horizon is set to be the following day, i.e. 24 h starting from the current time epoch. The day is then further divided into T time slots, each with a duration of 1 time unit, e.g. 1 h. The following assumptions are made:

- The base load accounting for the BCS operation is ignored. The total power consumption thus solely depends on the optimal aggregate charging rate of the entire BCS, solved by the OPD. Hence, from now on we focus particularly on the power dispatch to the CPS, as the RPS dispatch is simply deducting the CPS dispatch from the total.
- Due to the space and cost limitations, the RPS installed by an individual BCS should not be large in scale. This would make it suitable for a BCS to be located even in densely populated areas, such as the city centre.
- The marginal cost for renewable generation is ignored. The reason is that such a cost is mostly related to the initial inventory investment, instead of the charging operation considered in this work.
- No energy storage device other than the DBs being charged is required or considered in this study. This is to avoid too much energy being accumulated in a compact facility like a BCS since it is neither cost-efficient nor safe.
- All the power values concerned with the model, e.g. charging rate and renewable generation rate, are assumed to be constant within any single time slot. Hence, a power rating for one time slot is equal to the amount of energy consumed in the same time slot numerically, and we will thus use the power and energy terms interchangeably hereafter.
- The number of FBs that need to be available at a time epoch t is called the *FB demand* at t. They are specified on a per-hour basis in a contract. Hence, no FB demand exists at any other time epoch. Also each of them is *not* cumulative, i.e. excluding the FBs that should have been taken away before t.
- There are enough DBs in inventory to fulfil the FB demands throughout the coming day *before the day starts*. This is to allow for the highest scheduling flexibility.
- All batteries are homogeneous for the purpose of fulfilling the FB demands. This is reasonable considering that the plug-and-play interface is highly likely to be standardised in the near future.

In summary, we are interested in finding the optimal amounts of (i) purchased day-ahead grid power and (ii) the real-time aggregate charging rate of the BCS, in each time slot, respectively, so as to minimise the total expected charging cost.

2.2 System model

In this section, we consider firstly the model for the batteries, then that for the entire BCS, during any time slot $T_t = (t-1, t]$ for $t \in \{1, 2, \dots, T\}$.

2.2.1 Model for the batteries.: The FB demand at t is denoted by D_t. Meanwhile, the BCS may have some initial FB inventory F^{ini} at time epoch 0. Hence, we define the *cumulative new FB demand* at time epoch t as the minimum required total number of newly produced FBs *from the beginning of the day to t*, given by

$$F_t = \begin{cases} \max\left\{\sum_{\tau=1}^{t} D_\tau - F^{\text{ini}}, 0\right\} & t < T, \\ \sum_{\tau=1}^{T} D_\tau & t = T. \end{cases} \tag{1}$$

The case $t = T$ indicates that at the end of the scheduling horizon, the FB inventory should return to its initial state F^{ini}. This keeps the operation of the BCS stable and sustainable. As a result, all the required $\sum_{\tau=1}^{T} D_\tau$ FBs should be produced by the end of the day, but within the day some flexibility for charging scheduling is allowed. Since all the D_t and F^{ini} values are given, all the F_t's are directly obtainable and hence fixed. Note that for the first few time slots, if the initial F^{ini} FBs can already meet the FB demands, there may be no urgent need to produce new FBs, which justifies F_t's being lower-bounded by 0.

From the above definition, we can easily derive that at least F_T FBs are required to be produced throughout the day, and correspondingly the F_T DBs are already waiting in the DB inventory at time epoch 0 as assumed earlier.

For each individual DB $b \in \{1, 2, \dots, F_T\}$, denote s_b^{ini} as its initial SOC level in the unit of energy, known to the BCS operator a priori. (All units of power used in this paper are kW, and all units of energy are kWh, unless otherwise specified.) Each battery b also has an energy storage capacity, $s_b^{\max}$, perceived as readily available through a pre-screening step. We calculate the required amount of energy $(s_b^{\max} - s_b^{\text{ini}})/\eta_b$ by each DB b to become an FB, where η_b is its charging efficiency factor (given). Then we reorder the DBs in *ascending* order of this value. The DBs also follow the same order chronologically to be plugged into the CBs as well as to finish charging. Hence, suppose we want to get totally f new FBs since time epoch 0. The amount of energy that needs charging into the batteries should be no less than $\sum_{b=1}^{f}((s_b^{\max} - s_b^{\text{ini}})/\eta_b)$.

2.2.2 Model and constraints for the entire BCS.: Let R_t denote the constant *aggregate* charging rate over all the batteries staying in the CBs during time slot T_t. A DB may finish charging and become an FB at any time epoch (not merely limited to $t \in \{1, 2, \dots, T\}$) when another DB instantaneously replaces the FB in the CB and the latter enters the FB inventory immediately. This is reasonable with current techniques of doing so within several minutes [31] or even tens of seconds [32]. Then for all $t \in \{1, 2, \dots, T\}$, the total amount of energy charged into the batteries during $(0, t]$ should be no less than the cumulative energy demand so as to meet all the FB demand specifications. That is to say

$$\sum_{\tau=1}^{t} R_\tau \geq \sum_{b=1}^{F_t} \frac{s_b^{\max} - s_b^{\text{ini}}}{\eta_b} \quad \forall t \text{ s.t. } F_t > 0. \tag{2}$$

Additionally, the aggregate charging rate should be upper bounded, i.e.

$$0 \leq R_t \leq R^{\max} \quad \forall t, \tag{3}$$

where $R^{\max}$ is the upper bound in any time slot.

For any time slot T_t, use x_t to denote the amount of energy to be purchased from the CPS in day-ahead, and p_t^{DA} for the day-ahead market price for unit energy. Then the total day-ahead energy payment of the BCS is $\sum_{t=1}^{T} p_t^{\text{DA}} x_t$. The optimal values of x_t's, i.e. $x_t^\star$'s, are obtained by solving an optimisation problem discussed in the later sections.

In real-time, i.e. on the immediate day after the day-ahead purchasing request has been made, the aggregate charging rates at some time slots may differ from the generated renewable energy plus the day-ahead purchased grid energy, $\xi_t + x_t^\star$. Let the net *shortage* part be denoted as

$$a_t = R_t - \xi_t - x_t^\star . \tag{4}$$

Hence, when $a_t > 0$, this amount of energy should be purchased from the real-time market to support the optimal aggregate charging rate in T_t. This leads to an additional payment of $p_t^{\mathrm{RT,buy}} a_t$, where $p_t^{\mathrm{RT,buy}}$ is the real-time market unit price. On the other hand, if $a_t < 0$, i.e. when energy is already more than necessary in T_t without real-time purchase, the excess amount $-a_t$ can be sold back to the grid at the price of $p_t^{\mathrm{RT,sell}}$. (Note that this price is non-negative.) In this case, the payment is reduced by $-p_t^{\mathrm{RT,sell}} a_t$. Ideally, if the market is totally rational, the condition $0 \le p_t^{\mathrm{RT,sell}} \le p_t^{\mathrm{DA}} \le p_t^{\mathrm{RT,buy}}$ should hold, though this is not required as will be demonstrated in Section 4. There is also a battery degradation cost $\mathscr{C}^{\mathrm{B}}(R_t)$ introduced by charging the batteries at different charging rates during T_t. It is assumed to be a generic convex increasing function. Combining the above cases gives the total real-time charging cost as

$$\begin{aligned}\mathscr{C}^{\mathrm{RT}}(\mathbf{x}^\star, \boldsymbol{\xi}, \mathbf{R}) &= \sum_{t=1}^{T} \Big[a_t\big(p_t^{\mathrm{RT,buy}} \mathbb{I}[a_t > 0] + p_t^{\mathrm{RT,sell}} \mathbb{I}[a_t < 0]\big) \\ &\quad + \mathscr{C}^{\mathrm{B}}(R_t)\Big] \\ &= \sum_{t=1}^{T} \Big[\max\left\{p_t^{\mathrm{RT,buy}} a_t, p_t^{\mathrm{RT,sell}} a_t\right\} + \mathscr{C}^{\mathrm{B}}(R_t)\Big],\end{aligned} \tag{5}$$

where $\mathbf{x}^\star, \boldsymbol{\xi}$ and $\mathbf{R}$ are all T-dimensional vectors (all the vectors in this study are T-dimensional, unless otherwise specified), and

$$\mathbb{I}[\text{`statement'}] = \begin{cases} 1 & \text{if `statement' is true,} \\ 0 & \text{otherwise} \end{cases}$$

is the indicator function.

It is trivial that the net grid power flow, i.e. the purchased day-ahead power plus the real-time adjustment, can be obtained by subtracting the generated renewable power from the aggregate charging rate. Regardless of its sign, its magnitude should be upper bounded by the power line delivery capacity [33], which may be less than $R^{\max}$ so as to increase the power line utilisation. Moreover, the utility company may impose even stricter constraints with the hope that the BCS can provide some ancillary services for the grid, for example, frequency regulation. This yields

$$-x_t^{\max} \le R_t - \xi_t \le x_t^{\max} \quad \forall t, \tag{6}$$

where $x_t^{\max}$ is the resultant magnitude of the maximum power that can be drawn from or delivered back to the grid in T_t. As a special case, if there is no additional requirement from the utility side, we only consider the power line delivery capacity, which makes a constant $x_t^{\max} = x^{\max}\ \forall t$.

Finally, note that all the continuous decision variables are non-negative. Then we define the total minimum real-time payment of the BCS (excluding the day-ahead commitment already made), given a renewable generation profile $\boldsymbol{\xi}$, as

$$\begin{aligned}\mathscr{Q}(\mathbf{x}^\star, \boldsymbol{\xi}) = \min_{\mathbf{R} \ge \mathbf{0}} \quad & \mathscr{C}^{\mathrm{RT}}(\mathbf{x}^\star, \boldsymbol{\xi}, \mathbf{R}) \\ \text{s.t.} \quad & (2), (3), (6) .\end{aligned} \tag{7}$$

Hence, $\mathscr{Q}(\mathbf{x}^\star, \boldsymbol{\xi})$ is the minimal real-time cost, which is realised through a set of optimal aggregate charging rates $\mathbf{R}^\star$.

3 OPD problem formulation and solution

3.1 Problem formulation

From the previous subsection on describing the operation of a dual-source BCS, the OPD problem is formulated as

$$\begin{aligned}\min_{\mathbf{x} \ge \mathbf{0}} \quad & \sum_{t=1}^{T} p_t^{\mathrm{DA}} x_t + \mathbb{E}[\mathscr{Q}(\mathbf{x}, \boldsymbol{\xi})] \\ \text{s.t.} \quad & (2), (3), (6) .\end{aligned}$$

3.2 Solution to OPD

The above formulation essentially resembles the general framework of a two-stage stochastic optimisation problem [34]. In the first stage, since it is generally difficult to obtain a closed-form expression of $\mathbb{E}[\mathscr{Q}(\mathbf{x}, \boldsymbol{\xi})]$, the SAA method is often deployed to approximate the expectation term in practice [35]. In particular, N sample realisations of $\boldsymbol{\xi}$, $\{\boldsymbol{\xi}^1, \boldsymbol{\xi}^2, \ldots, \boldsymbol{\xi}^n, \ldots, \boldsymbol{\xi}^N\}$, are generated, and the problem is converted to the following form:

$$\begin{aligned}\min_{\mathbf{x}, \mathbf{R}^n \ge \mathbf{0}\ \forall n} \quad & \sum_{t=1}^{T} p_t^{\mathrm{DA}} x_t + \frac{1}{N} \sum_{n=1}^{N} \mathscr{C}^{\mathrm{RT}}(\mathbf{x}, \boldsymbol{\xi}^n, \mathbf{R}^n) \\ \text{s.t.} \quad & \sum_{\tau=1}^{t} R_\tau^n \ge \sum_{b=1}^{F_t} \frac{s_b^{\max} - s_b^{\mathrm{ini}}}{\eta_b} \quad \forall t, n \\ & 0 \le R_t^n \le R^{\max} \quad \forall t, n \\ & -x_t^{\max} \le R_t^n - \xi_t^n \le x_t^{\max} \quad \forall t, n,\end{aligned}$$

where $\mathbf{R}^n$ corresponds to the optimal solution to $\mathscr{Q}(\mathbf{x}, \boldsymbol{\xi}^n)$. Hereafter, this formulation is referred to as **OPD-I**. When the number of constructed scenarios, N, is large enough, the second summation term would be adequate to approximate the expectation on average according to the law of large numbers [34]. However, N cannot be excessively large due to the curse of dimensionality. Note that at this point we do not have knowledge about the actual RTP realisation yet, so the $p_t^{\mathrm{RT,buy}}$'s and $p_t^{\mathrm{RT,sell}}$'s that are plugged into the first-stage calculation are estimated values from historical data, achievable by methods such as [36].

In the second stage, $\mathbf{x}^\star$, the optimal solution to OPD-I, is regarded as fixed. Usually, at the beginning of the day we can obtain the precise realisation of renewable energy generation process or at least a more accurate version than we can do based on historical data only. This can be achieved by various means [37, 38]. As a result, $\boldsymbol{\xi}$ is also fixed to $\hat{\boldsymbol{\xi}}$, and denote

$$\hat{a}_t = R_t - \hat{\xi}_t - x_t^\star . \tag{8}$$

Also note that the *actual* RTP information, $\hat{\mathbf{p}}_t^{\mathrm{RT,buy}}$ and $\hat{\mathbf{p}}_t^{\mathrm{RT,sell}}$, is announced by the utility at this time. Then we derive the optimal charging schedule by solving the following problem:

$$\begin{aligned}\min_{\mathbf{R} \ge \mathbf{0}} \quad & \sum_{t=1}^{T} \Big[\max\left\{\hat{p}_t^{\mathrm{RT,buy}} \hat{a}_t, \hat{p}_t^{\mathrm{RT,sell}} \hat{a}_t\right\} + \mathscr{C}^{\mathrm{B}}(R_t)\Big] \\ \text{s.t.} \quad & (2), (3), \\ & -x_t^{\max} \le R_t - \hat{\xi}_t \le x_t^{\max} \quad \forall t .\end{aligned}$$

However, it is impractical to obtain complete and accurate (or actual) RTP and renewable generation information at the beginning of the day. Only the RTP and the amount of generated renewable energy for the current time slot are known. As a result, we propose to attack the second-stage problem using a shrinking window approach for the scheduling horizon. That means, at each time slot T_t $(t < T)$, we only have $\hat{p}_t^{\mathrm{RT},\cdot}$ and $\hat{\xi}_t$ as the actual RTP and renewable generation, and $p_\tau^{\mathrm{RT},\cdot}$ and $\xi_\tau\ \forall \tau \in \{t+1, \ldots, T\}$ are still from the predicted values in day-ahead. Those time slots before T_t do not need to be considered, as the decisions made already cannot be improved. Then for each $t \in \{1, 2, \ldots, T-1\}$ we solve the problem iteratively:

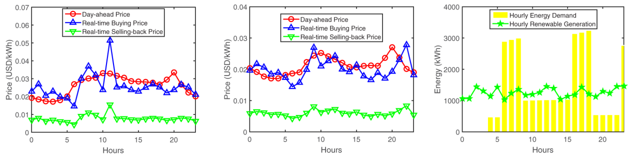

a b c

Fig. 2 *Simulation setup*
(a) Electricity price for weekdays, ***(b)*** Electricity price for weekends, ***(c)*** Hourly energy demands and renewable generation

$$
\begin{aligned}
\min_{\mathbf{R}^{(t)} \geq \mathbf{0}} \quad & \left[\max\left\{ \hat{p}_t^{\text{RT,buy}} \hat{a}_t, \hat{p}_t^{\text{RT,sell}} \hat{a}_t \right\} + \mathscr{C}^{\text{B}}(R_t) \right] \\
& + \sum_{\tau = t+1}^{T} \left[\max\left\{ p_\tau^{\text{RT,buy}} a_\tau, p_\tau^{\text{RT,sell}} a_\tau \right\} + \mathscr{C}^{\text{B}}(R_\tau) \right] \\
\text{s.t.} \quad & (2), (3), \\
& -x_t^{\max} \leq R_t - \hat{\xi}_t \leq x_t^{\max}, \\
& -x_\tau^{\max} \leq R_\tau - \xi_\tau \leq x_\tau^{\max} \quad \forall \tau \in \{t+1, \ldots, T\},
\end{aligned}
$$

where $\mathbf{R}^{(t)} = [R_t \quad \cdots \quad R_T]$ is a $(T - t + 1)$-dimensional temporary variable holding the best guesses for the charging rates in the current and future time slots based on currently available information. The first entry of $\mathbf{R}^{(t)\star}$, the optimal solution for the tth iteration, would be the decision taken for the current time slot, whereas the rest are discarded. Certainly, when $t = T$, the problem becomes

$$
\begin{aligned}
\min_{R_T \geq 0} \quad & \max\left\{ \hat{p}_T^{\text{RT,buy}} \hat{a}_T, \hat{p}_T^{\text{RT,sell}} \hat{a}_T \right\} + \mathscr{C}^{\text{B}}(R_T) \\
\text{s.t.} \quad & (2), (3), \\
& -x_T^{\max} \leq R_T - \hat{\xi}_T \leq x_T^{\max}
\end{aligned}
$$

as a special case where $\mathbf{R}^{(T)} = R_T$. In other words, if $\mathbf{R}^\star$ is denoted as the optimal solution for the entire second-stage problem, then

$$
R_t^\star = R_1^{(t)\star} \quad \forall t. \tag{9}
$$

This iterative formulation will be referred to as **OPD-II** from now on.

After solving the optimal $\mathbf{R}^\star$, the BCS operator can know how to submit the real-time adjustment requests to the utility by

$$
\hat{a}_t^\star = R_t^\star - \hat{\xi}_t - x_t^\star \quad \forall t. \tag{10}
$$

This gives a final total charging cost for the entire scheduling horizon as

$$
\mathscr{C}^\star = \sum_{t=1}^{T} \left\{ p_t^{\text{DA}} x_t^\star + \left[\max\left\{ \hat{p}_t^{\text{RT,buy}} \hat{a}_t^\star, \hat{p}_t^{\text{RT,sell}} \hat{a}_t^\star \right\} + \mathscr{C}^{\text{B}}(R_t^\star) \right] \right\}. \tag{11}
$$

4 Numerical simulation

4.1 Simulation setup

This subsection will cover the data sources and parameters for validation of our OPD algorithm. All of the conditions illustrated here will be referred to as the *base conditions* unless otherwise specified.

4.1.1 Scheduling horizon.: One day, with each time slot being one hour.

4.1.2 Costs.: The day-ahead and real-time buying market pricing data, $\mathbf{p}^{\text{DA}}$ and $\mathbf{p}^{\text{RT,buy}}$, are from NYISO [39], and the real-time selling-back market pricing data is determined by $\mathbf{p}^{\text{RT,sell}} = 0.3\mathbf{p}^{\text{RT,buy}}$. All of them are in 1-h granularity. We select the patterns for Wednesdays and Saturdays to represent a typical weekday and weekend, respectively, and plot them in Figs. 2*a* and *b*. The RTP curves are from five consecutive weeks' average to reduce randomness of the real market. We also assume that for the base conditions, we have accurate prediction on RTP, which leads to $\hat{\mathbf{p}}^{\text{RT,buy}} = \mathbf{p}^{\text{RT,buy}}$ and $\hat{\mathbf{p}}^{\text{RT,sell}} = \mathbf{p}^{\text{RT,sell}}$. Note that for real data, the ideal condition $0 \leq p_t^{\text{RT,sell}} \leq p_t^{\text{DA}} \leq p_t^{\text{RT,buy}}$ does not have to always hold, which is indeed violated several times in the data used here. However, this will not affect the correctness of our algorithm as long as we know the relative comparison among the three curves, illustrated later through simulation.

As for the battery degradation, for simplicity, the cost function follows a quadratic form, i.e. $\mathscr{C}^{\text{B}}(R_t) = c^{\text{B}} R_t^2$, where c^{B} is a cost factor to link the charging rate to the degradation cost per unit time. Here we set it to be 5 USD $\cdot$ $(\text{MW})^{-2}$.

4.1.3 Parameters for the batteries.: Each battery has a storage capacity of $s_b^{\max} = 100$ kWh, with a charging efficiency of $\eta_b = 0.9\ \forall b$. The initial SOC of each battery, s_b^{ini}, is randomly generated from a uniform distribution in $[0, 15]$ kWh.

4.1.4 Parameters for the BCS.: The BCS has 50 CBs to support simultaneous charging of multiple DBs. The maximum allowed charging rate for each CB is set to $r_l^{\max} = 100$ kW $\forall l$. Hence, we can simply set $R^{\max} = 5000$ kW. At the beginning of the day, there are $F^{\text{ini}} = 20$ initial FBs in the inventory. The FB demand at the end of each hour follows this pattern:

$$
D_t = \begin{cases} D_{\text{valley}}, & 1 \leq t \leq 6 \ \text{ or } \ 20 \leq t \leq 24, \\ D_{\text{normal}}, & 10 \leq t \leq 16, \\ D_{\text{peak}}, & \text{otherwise}, \end{cases} \tag{12}
$$

where the meanings of the three demand values are self-explanatory. Typically, $0 \leq D_{\text{valley}} \leq D_{\text{normal}} \leq D_{\text{peak}}$. Here, $D_{\text{peak}} = 30$ per hour for the peak hours of 7–9 am and 5–7 pm, $D_{\text{normal}} = 10$ per hour for the normal hours of 10 am–4 pm, and $D_{\text{valley}} = 5$ per hour for the remaining valley hours. Resultantly, the hourly energy demands can be computed and plotted as the yellow bars in Fig. 2*c*. The bars' heights are increasing even for hours with identical FB demands since we have presorted the DBs' energy demands as mentioned in Section 2.2.1. The grid power line transmission capacity is set to $x_t^{\max} = 4000$ kW $\forall t$, assuming that the utility does not impose an additional requirement for the BCS to provide ancillary services. Note that we have $x_t^{\max} < R^{\max}$ here.

4.1.5 Renewable generation.: The generation rate of the RPS, ξ_t, is uniformly distributed in $[1000, 1500]$ kW to simulate an average wind turbine [40]. $N = 100$ scenarios are generated when performing the SAA. For fair comparisons between runs, instead of generating a new realisation of renewable generation for the second stage of each run, the sample paths have a fixed pattern as depicted by the green curve in Fig. 2*c*. Certainly it is not fed into the first stage to prevent cheating.

4.1.6 Runtime environment.: The algorithm is implemented using CVX [41, 42] in MATLAB R2015a on a Windows 10 PC with a 3.20 GHz Intel Core i5 quad-core CPU and 8 GB RAM.

4.2 Results and discussion

4.2.1 Charging cost reduction.: We compare our proposed OPD with a benchmark algorithm, which

- Does no day-ahead commitment.
- Uses up all renewable energy generated before purchasing real-time grid power.
- Charges DBs at the fastest rate.
- Sells back excess renewable energy if any.

From the resultant CPS dispatch depicted in Figs. 3*a* and *b*, under the base conditions for both weekdays and weekends, the

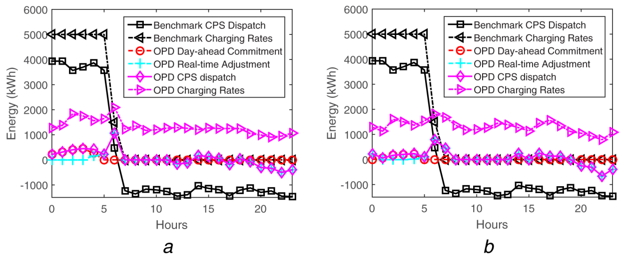

Fig. 3 *Power dispatch under the base conditions*
(a) Power dispatch on a weekday, ***(b)*** Power dispatch on a weekend

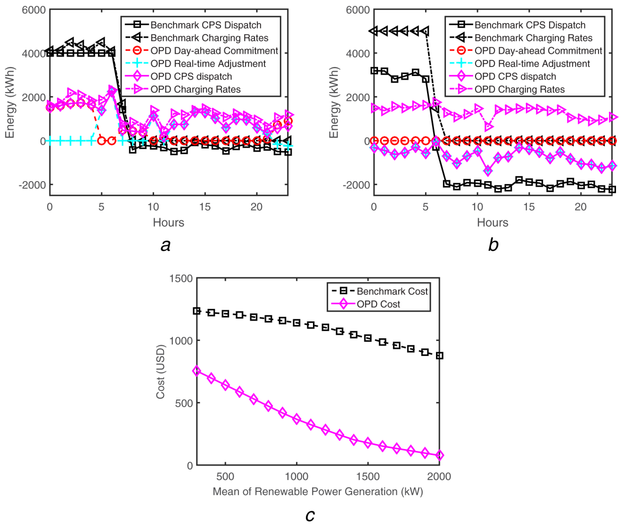

Fig. 4 *Impact of renewable generation*
(a) Power dispatch when $\bar{\xi} = 300\,\text{kW}$, ***(b)*** Power dispatch when $\bar{\xi} = 2000\,\text{kW}$, ***(c)*** Total charging cost w.r.t. renewable generation

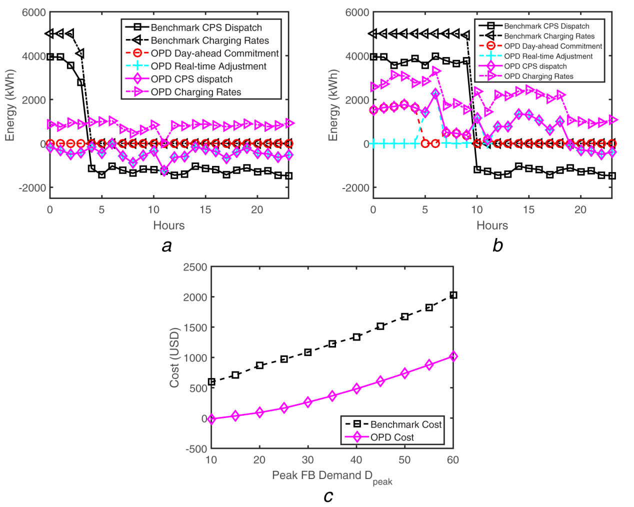

Fig. 5 *Impact of FB demands*
(a) Power dispatch when $D_{\text{peak}} = 10$ per hour, ***(b)*** Power dispatch when $D_{\text{peak}} = 60$ per hour, ***(c)*** Total charging cost w.r.t. peak FB demands

benchmark simply finishes charging at the very beginning and stays idle in the remaining time. The available information on renewable generation and RTP is apparently not fully utilised. On the other hand, our proposed OPD is able to adapt the charging rates intelligently to minimise the overall cost. Note that under the settings in Section 4.1.5, the RPS dispatches are always the same over all base condition simulations, so we only plot the CPS dispatch curves.

The charging costs under both algorithms are listed in the first two data rows of Table 1. Based on accurately predicted RTPs, our OPD beats the benchmark scheme with a cost saving of 76%. This is thanks to utilising the (supposedly often) cheaper day-ahead market as well as the (zero-cost) renewable energy as much as possible.

Table 1 Charging cost saving and load balancing capability of OPD

Metric	OPD	Benchmark
Charging cost (weekday) (USD)	262.11	1087.77
Charging cost (weekend) (USD)	252.61	1073.17
PAR (weekday)	1.59	3.81
PAR (weekend)	1.39	3.81

4.2.2 Load balancing capability.: We compute the peak-to-average ratio (PAR) of the charging rate under both schemes, with the results shown in the third and fourth data rows of Table 1. The PARs for the OPD on both days are much lower than those for the benchmark scheme because our OPD is more effective in utilising the more economical power source adaptively while the benchmark scheme is prone to real-time fluctuations in both renewable generation and price. Also, the average absolute CPS dispatch is 317.86 kW under OPD, and 1816.5 kW under the benchmark. Both facts indicate that our OPD not only reduces battery degradation due to high charging rates but also relieves the burden on the grid. In return, the utility companies would have more incentive to support the adoption of the battery swapping mode.

4.2.3 Robustness.: Note that at $t = 5, 6$ or 10, $p_t^{\text{DA}} > p_t^{\text{RT,buy}}$. During those hours, the day-ahead commitments become zero, and all the conventional power required for those hours is from the real-time market, as depicted in Fig. 3. This shows that our OPD is always feasible regardless of whether the market is ideal or not, as long as the pricing irrationality (e.g. that the day-ahead price is sometimes higher than that in real-time) is successfully forecast.

4.2.4 Impact of renewable generation.: For the remaining discussions, we will use only the weekday setting as the base condition. Firstly, the mean value of renewable power output, denoted by $\bar{\xi}$, is altered between 300 kW and 2000 kW with the peak-to-peak amplitude fixed at 500 kW. Two sample dispatches for $\bar{\xi} = 300\,\text{kW}$ and 2000 kW, respectively, are plotted in Figs. 4*a* and *b*. The saving (i.e. the gap in Fig. 4*c*) is intuitively more obvious with higher renewable penetration. This should encourage BCS operators to consider integrating renewables in their facilities.

4.2.5 Impact of FB demands.: We fix the FB demands for the valley and normal periods, and alter the peak period demand D_{peak} from 10 to 60 per hour. The resultant dispatches under $D_{\text{peak}} = 10, 30$ and 60 are illustrated in Figs. 5*a*, 3*a* and 5*b*, respectively. From Fig. 5*c*, the cost saving of the OPD compared with the benchmark scheme is more evident with higher FB demands. This is a valuable result for a busy BCS serving multiple BSSs of probably the whole metropolis, which would be the typical situation after popularisation of EVs.

5 Conclusion and future work

This work has studied the OPD problem for a dual-source centralised EV BCS. The formulation aims at finding the cost-minimal power dispatch to the CPS and the RPS subject to satisfaction of the specified FB demands. We formulate the OPD as a two-stage stochastic optimisation problem and solve it using SAA. The formulation is simple yet capable of capturing the fundamental physical constraints, and the convergence is reasonably fast on an average PC. Numerical simulations using real price data have been presented to validate the proposed OPD model and demonstrated the effectiveness of the algorithm with regard to some affecting factors.

The formulation allows for many potential extensions. For instance, currently, the FB demands and individual battery parameters are perceived as given. If the DB arrival is also stochastic, the model can be updated with a more flexible representation of the minimum required energy. Moreover, bidirectional charging (i.e. allowing both charging and discharging of the batteries) is essential to enabling battery-to-grid service [43]. This is an important component of ancillary service such as frequency regulation [44] but has not been discussed in this study. We also leave the more theoretical proofs, such as the performance bound, as future work of this application-driven paper.

6 References

[1] Richardson, D.B.: 'Electric vehicles and the electric grid: a review of modeling approaches, impacts, and renewable energy integration', *Renew. Sustain. Energy Rev.*, 2013, **19**, pp. 247–254

[2] Mwasilu, F., Justo, J.J., Kim, E.K., *et al.*: 'Electric vehicles and smart grid interaction: a review on vehicle to grid and renewable energy sources integration', *Renew. Sustain. Energy Rev.*, 2014, **34**, pp. 501–516

[3] Shahan, Z.: 'China electric bus sales still exploding—CleanTechnica', 2017. Available at https://cleantechnica.com/2017/02/25/china-electric-buses-still-exploding/

[4] Kane, M.: 'BYD scores Europe's largest electric bus fleet order', 2015. Available at http://insideevs.com/byd-scores-europes-largest-electric-bus-fleet-order/

[5] 'Tesla—premium electric sedans and SUVs', 2017. Available at https://www.tesla.com/

[6] 'e6, pure electric car—auto—BYD', Available at http://www.byd.com/la/auto/e6.html

[7] Wang, R., Wang, P., Xiao, G.: 'Two-stage mechanism for massive electric vehicle charging involving renewable energy', *IEEE Trans. Veh. Technol.*, 2016, **65**, (6), pp. 4159–4171

[8] Yilmaz, M., Krein, P.T.: 'Review of battery charger topologies, charging power levels, and infrastructure for plug-in electric and hybrid vehicles', *IEEE Trans. Power Electron.*, 2013, **28**, (5), pp. 2151–2169

[9] Dong, Q., Niyato, D., Wang, P., *et al.*: 'The PHEV charging scheduling and power supply optimization for charging stations', *IEEE Trans. Veh. Technol.*, 2016, **65**, (2), pp. 566–580

[10] Tan, X., Sun, B., Tsang, D.H.K.: 'Queueing network models for electric vehicle charging station with battery swapping'. 2014 IEEE Int. Conf. on Smart Grid Communications (SmartGridComm), 2014, pp. 1–6

[11] Dincer, I., Hamut, H.S., Javani, N.: '*Thermal management of electric vehicle battery systems*' (Automotive Series, Wiley, Chichester, 2017)

[12] Mak, H.Y., Rong, Y., Shen, Z.J.M.: 'Infrastructure planning for electric vehicles with battery swapping', *Manage. Sci.*, 2013, **59**, (7), pp. 1557–1575

[13] Cheng, L., Chang, Y., Lin, J., *et al.*: 'Power system reliability assessment with electric vehicle integration using battery exchange mode', *IEEE Trans. Sustain. Energy*, 2013, **4**, (4), pp. 1034–1042

[14] Miao, Y., Jiang, Q., Cao, Y.: 'Battery switch station modeling and its economic evaluation in microgrid'. 2012 IEEE Power and Energy Society General Meeting, 2012, pp. 1–7

[15] Tumuluru, V.K., Tsang, D.H.K.: 'A two-stage approach for network constrained unit commitment problem with demand response', *IEEE Trans. Smart Grid*, 2016

[16] Wu, Y., Tan, X., Qian, L., *et al.*: 'Optimal pricing and energy scheduling for hybrid energy trading market in future smart grid', *IEEE Trans. Ind. Inf.*, 2015, **11**, (6), pp. 1585–1596

[17] Wu, Y., Lau, V.K.N., Tsang, D.H.K., *et al.*: 'Optimal energy scheduling for residential smart grid with centralized renewable energy source', *IEEE Syst. J.*, 2014, **8**, (2), pp. 562–576

[18] Agheb, S., Tan, X., Sun, B., *et al.*: 'Robust provisioning of demand-side flexibility under electricity price uncertainty'. 2016 IEEE Int. Conf. on Industrial Technology (ICIT), 2016, pp. 545–550

[19] Maharjan, S., Zhang, Y., Gjessing, S., *et al.*: 'User-centric demand response management in the smart grid with multiple providers', *IEEE Trans. Emerg. Top. Comput.*, 2017, **5**, (4), pp. 494–505

[20] Zhang, K., Mao, Y., Leng, S., *et al.*: 'Platoon-based electric vehicles charging with renewable energy supply: a queuing analytical model'. 2016 IEEE Int. Conf. Communications (ICC), 2016, pp. 1–6

[21] Raviv, T.: 'The battery switching station scheduling problem', *Oper. Res. Lett.*, 2012, **40**, (6), pp. 546–550

[22] Schneider, F., Thonemann, U.W., Klabjan, D.: 'Optimization of battery charging and purchasing at electric vehicle battery swap stations', *Transp. Sci.*, to be published

[23] Sun, B., Tan, X., Tsang, D.: 'Optimal charging operation of battery swapping and charging stations with QoS guarantee', *IEEE Trans. Smart Grid*, to be published

[24] Zhang, M., Chen, J.: 'The energy management and optimized operation of electric vehicles based on microgrid', *IEEE Trans. Power Deliv.*, 2014, **29**, (3), pp. 1427–1435

[25] Zhang, T., Chen, W., Han, Z., *et al.*: 'Charging scheduling of electric vehicles with local renewable energy under uncertain electric vehicle arrival and grid power price', *IEEE Trans. Veh. Technol.*, 2014, **63**, (6), pp. 2600–2612

[26] Jin, C., Sheng, X., Ghosh, P.: 'Optimized electric vehicle charging with intermittent renewable energy sources', *IEEE J. Sel. Top. Signal Process.*, 2014, **8**, (6), pp. 1063–1072

[27] Qian, L.P., Zhang, Y.J.A., Huang, J., *et al.*: 'Demand response management via real-time electricity price control in smart grids', *IEEE J. Sel. Areas Commun.*, 2013, **31**, (7), pp. 1268–1280

[28] Tumuluru, V.K., Huang, Z., Tsang, D.H.K.: 'Integrating price responsive demand into the unit commitment problem', *IEEE Trans. Smart Grid*, 2014, **5**, (6), pp. 2757–2765

[29] Tan, X., Wu, Y., Tsang, D.H.K.: 'Pareto optimal operation of distributed battery energy storage systems for energy arbitrage under dynamic pricing', *IEEE Trans. Parallel Distrib. Syst.*, 2016, **27**, (7), pp. 2103–2115

[30] Tan, X., Wu, Y., Tsang, D.H.K.: 'A stochastic shortest path framework for quantifying the value and lifetime of battery energy storage under dynamic pricing', *IEEE Trans. Smart Grid*, 2017, **8**, (2), pp. 769–778

[31] Contact, P.: 'Battery swapping becoming common practice for commercial vehicles—Electronics News', 2013. Available at https://electronicsnews.com.au/battery-swapping-becoming-common-practice-for-commercial-vehicles/

[32] Bullis, K.: 'Why Tesla thinks it can make battery swapping work - MIT Technology Review', 2013. Available at https://www.technologyreview.com/s/516276/why-tesla-thinks-it-can-make-battery-swapping-work/

[33] Sun, B., Huang, Z., Tan, X., *et al.*: 'Optimal scheduling for electric vehicle charging with discrete charging levels in distribution grid', *IEEE Trans. Smart Grid*, to be published

[34] Shapiro, A., Philpott, A.: 'A tutorial on stochastic programming', Manuscript, 2007. Available at http://www2.isye.gatech.edu/people/faculty/Alex_Shapiro/TutorialSP.pdf

[35] Kleywegt, A.J., Shapiro, A., de Mello, T.H.: 'The sample average approximation method for stochastic discrete optimization', *SIAM J. Optim.*, 2002, **12**, (2), pp. 479–502

[36] Tan, Z., Zhang, J., Wang, J., *et al.*: 'Day-ahead electricity price forecasting using wavelet transform combined with ARIMA and GARCH models', *Appl. Energy*, 2010, **87**, (11), pp. 3606–3610

[37] Liu, H., Tian, H.Q., Chen, C., *et al.*: 'A hybrid statistical method to predict wind speed and wind power', *Renew. Energy*, 2010, **35**, (8), pp. 1857–1861

[38] Liu, S., Lu, J., Wu, Q., *et al.*: 'Harvesting-aware power management for real-time systems with renewable energy', *IEEE Trans. Very Large Scale Integration (VLSI) Syst.*, 2012, **20**, (8), pp. 1473–1486

[39] 'Nyiso (markets & operations - market data - pricing data)', 2016. Available at http://www.nyiso.com/public/markets_operations/market_data/pricing_data/index.jsp

[40] 'National wind watch—output from industrial wind power', 2016. Available at https://www.wind-watch.org/faq-output.php

[41] Grant, M., Boyd, S.: 'CVX: Matlab software for disciplined convex programming, version 2.1'. 2014. http://cvxr.com/cvx.

[42] Grant, M., Boyd, S.: 'Graph implementations for nonsmooth convex programs', in Boyd, V., Kimura, S., Blondel, H. (Eds.): '*Recent advances in learning and control. Lecture Notes in Control and Information Sciences*' (Springer-Verlag Limited, London, 2008), pp. 95–110. http://stanford.edu/~boyd/graph_dcp.html

[43] Farzin, H., Aghtaie, M., Fotuhi, M., *et al.*: 'Reliability studies of distribution systems integrated with electric vehicles under battery-exchange mode', *IEEE Trans. Power Deliv.*, 2016, **31**, (6), pp. 2473–2482

[44] Liu, H., Hu, Z., Song, Y., *et al.*: 'Vehicle-to-grid control for supplementary frequency regulation considering charging demands', *IEEE Trans. Power Syst.*, 2015, **30**, (6), pp. 3110–3119